Fig. 3.23. Close up of hotel damage. Relative ground movement, due to liquefaction, between the columns of the exterior roof structure and the building, caused the cracks.

3.4. Tambo de Mora

Tambo de Mora district, part of Chincha province in the Ica region, has a population of 5348 [4]. The city is located some 38 km from the USGS estimated epicenter, and 175 km south of the capital Lima. Buildings, industrial and public facilities in Tambo de Mora were severely damaged due to liquefaction induced ground failure and lateral spreading. To evaluate ground conditions we performed microtremor measurements at 8 locations.

Under the program of Sustainable Cities, INDECI in association with the National University of Ica [15] present the Seismic Hazard of Chincha city (see Fig. 3.24). According to the hazard zoning map, Tambo de Mora (Zone 1) has the highest risk in the area.

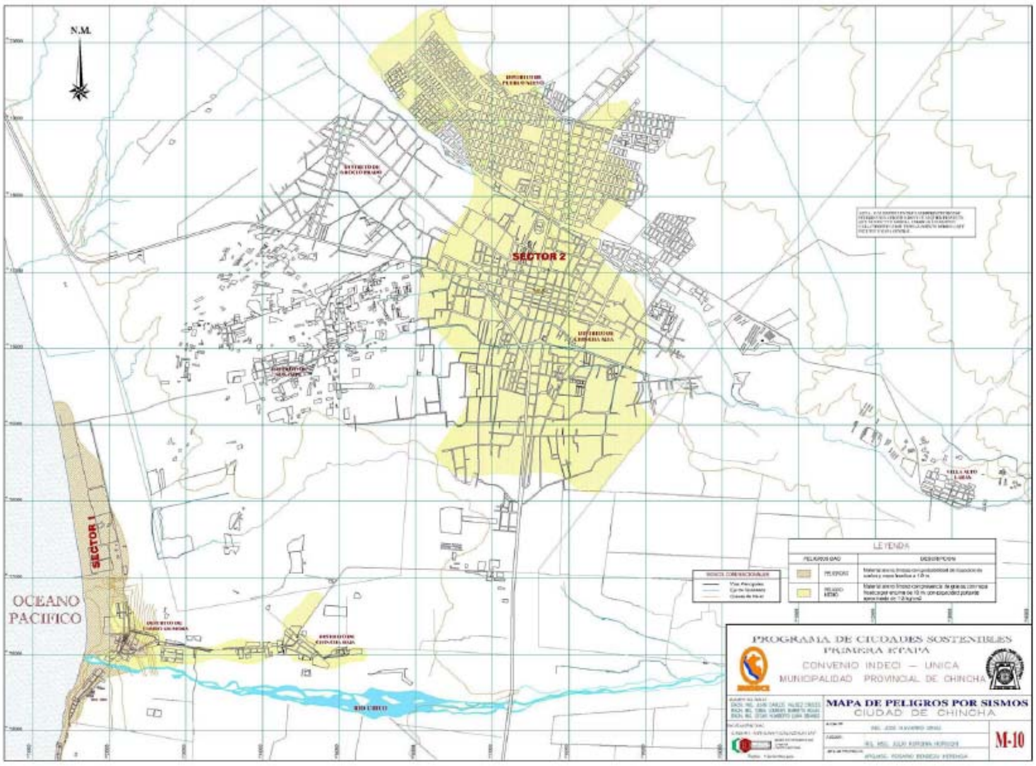

Fig. 3.24. Seismic Hazard Areas City of Chincha. INDECI [1]. Brown colored area next to the ocean indicates "dangerous"s area.

3.4.1. Damage

Severe settlement of buildings and foundation damage, due to liquefaction induced ground failure and lateral spreading, caused the collapse of adobe houses and severe cracking of walls of confined masonry buildings. The damage resulted in the death of 5 persons; Out of 1447 dwellings, 465 houses were completely destroyed, 308 were severely affected, another 467 were affected, and 121 were lightly affected [4]. This left only 121 unaffected houses.

Fig. 3.25. Settlement of 0.7 m of building in front of palm tree.

At Canchamana in the northern part of Tambo de Mora (0.5 km north of microtremor point 1.), a masonry community building (see Fig. 3.26) was severely damaged by lateral spreading and an adobe school building was partially collapsed, while a newer school building with proper foundation behaved well (Fig. 3.27.)

Fig. 3.26. Severely damaged community building in Canchamana, with liquefaction traces in the foreground.

Fig. 3.27. Severely damaged community building in Canchamana, with liquefaction traces in the foreground and well behaved red school building in the background.

Fig. 3.28. Foundation pushed up due settlement the building.

Fig. 3.29. Liquefaction splashed all the way to the top of Prison building door.

It is worthy to mention that Chincha Prison, located in the North of Tambo de Mora, suffered extensive damage due to liquefaction. The surrounding wall collapsed (see Fig. 3.30) and the prison cells exhibited large settlements (see prFig. 3.31). Due to the risk of additional damages, the local government decided to set free the prisoners. This fact suggests that location of this public building deserve further review as long as the social consequences of its failure were also considerable.

Fig. 3.30. Collapsed wall at Chincha prison due to large ground deformation

prFig. 3.31. Sand inside prison cell. (Courtesy of Julio Kuroiwa)

3.4.2. Geology and liquefaction

Tambo de Mora is located on an alluvial deposit in the south and a marine deposit in the north (see Fig. 3.32) and to the east of the marine deposit lies the Pleistocene Canete formation consisting of alternating layers of sand and silt stones [1]. Ground water level is very shallow in the marine deposit, surfacing at some locations. South of the river Chico, we found one well, close to microtremor point 8, where the water level was at approximately 2.5 meter.

Fig. 3.32. Google earth image of microtremor measurement locations and results.

In the northern part (close to Microtremor point 1) a lot of over 20 meter long cracks with grayish sand ejecta were observed. Cracks and up to 3 meter differential settlements (see Fig. 3.33) where seen closer to the Canete formation. Here light brown/beige seemingly liquefied soil covered parts of some of the vertical scarps. The liquefied area extends from the central park (Plaza de Armas) of Tambo de Mora all the way to Pan-American highway in the north, which is distance of more than 7 km. A large block moved seemingly had moved downwards from the Canete formation and this movement downward continued as marked by the dashed lines as seen in Fig. 3.34. However there was vegetation between the block and the slope so this movement did not happen in the 2007 earthquake.

Fig. 3.33. On the border between the Canete formation and the marine deposit, there is a 3 meter differential vertical offset.

Fig. 3.34. Block moved seemingly moved down and towards ocean some 5 meters, however there was vegetation between the block and the slope, so this did not happen in the 2007 earthquake.

3.4.3. Microtremor measurements

We measured microtremors in the afternoons of the September 18 and 19 at 8 locations from Canchamana in the North to San Pablo in the south (see Fig. 3.32). We used a Geodas-10 system with a velocity meter CR4.5-2SV, frequency range 0.5-20

Hz. The Sampling frequency was 100Hz, record length 2x3min or more and the software Geopsy [2] was used for data processing.

The result indicates that fundamental frequency increases from 3 Hz in the south to 5 Hz at “Plaza de Armas” and at point 8, south of the river, the frequency was approximately 12 Hz.

The microtremor results seem to be related to the geological conditions in that the lower fundamental frequencies are observed in the area of the marine deposit at location where water level is very close to or at the surface, and when moving south towards the stiffer alluvial deposit the frequencies increases to 5 Hz. The observed damage, in Tambo de Mora and other locations with marine deposits, such as Villa Swamps, port of Pisco and the port of Paracas, indicates that liquefaction resistant foundations, such as stiff reinforced foundations are necessary to avoid damages under similar conditions.

3.5. Pisco

3.5.1. Overview

Pisco, located 351 km south of Lima and 17 m AMSL, is the capital of the Pisco Province which belongs to the Ica Region. Initially funded in 1640, the city of Pisco was shifted to its current location during the period 1689-1705, in order to protect the city from pirates’ attacks and earthquakes in the late 16th century.

The city of Pisco has a population of about 54 192 according to the Census of 2005. It occupies an area of approximately 24.56 km², in a subtropical arid region of rainfalls ranging between scarce and null [7], having an average annual precipitation of 1.6 mm. In terms of economy, cotton processing factories, wineries, agriculture, fishing industries and other port-related businesses, are the most relevant.

Pisco is located directly above the central part of the estimated fault plane and a local intensity of 8.0 (MSK-64) was preliminarily estimated by Astroza [8]. According to the National Institute of Civil Defense (INDECI) the death toll in the city was 338, 70% of the whole earthquake dead toll, as of October 10, 2007 [11].

3.5.2. Geology

The geology of Pisco can be divided into two main formations [17]. One is Formation Pisco, a lithologic sequence of white color composed of diatomite with intercalation of tuff sandstones and shales, located between Pisco River and the surroundings of Camana. The other is the recent quaternary deposit, composed of clastic materials transported by water and then deposited on the river beds as coarse conglomerates intercalated with sand, silt and clay. These deposits can be observed along the river side and the terraces’ foot.

3.5.3. Early studies

The Japan-Peruvian Centre of Seismic Investigations and Disaster Mitigation (CISMID) of the National University of Engineering in Lima [13] carried out a detailed subsoil investigation, consisting of 25 trenches and 17 boreholes, for the city in 1998. The study aimed at mapping the distribution of soil types and their shear strength characteristics, identifying potentially liquefiable areas and quantifying the distribution of bearing capacity based on the usual foundation geometry used by locals. The field information collected in this study was enriched with data from even earlier studies.

Fig. 3.35 shows the proposed geotechnical zonation based on bearing capacity. The characteristics of each zone can be briefly described as:

- Zone I: Southwest of Pisco. A 0.2 m thick layer of fill material composed of clay and round gravels, overlying gravel poorly graded (GP), maximum size of 12", 22% of sand and 1.5% of non plastic and slightly wet fines. No phreatic level was identified. Bearing capacity ranges from 2.5 to 3.0 kgf/cm² (Df=0.8 m).
- Zone II: Northern and central coast of Pisco. 0.5 m of sandy clay layer overlying fine silty sand with a thickness of 1.1 m, followed by poorly graded gravel (GP). The phreatic level was found northwards at a depth of 1.4 m. The estimated bearing capacity was 2.0 Kgf/cm² (Df=1.1 m)
- Zone III: Central Pisco. 1.2 m of sandy clay layer overlying fine silty sand up to depths between 2.0 to 4.25 m, followed by gravel poorly graded (GP). The phreatic level is located between depths ranging from 1.0 to 1.8 m. The estimated bearing capacity was 1.0 Kgf/cm² (Df=0.8 m)
- Zone IV: Southeast of Pisco. 0.8 to 1.2 m of filling material composed of clay mixed with rounded gravel and debris deposits. Phreatic level was not observed and the bearing capacity was estimated to range between 2.0 and 2.5 kgf/cm² (Df=0.8-1.2 m).
-

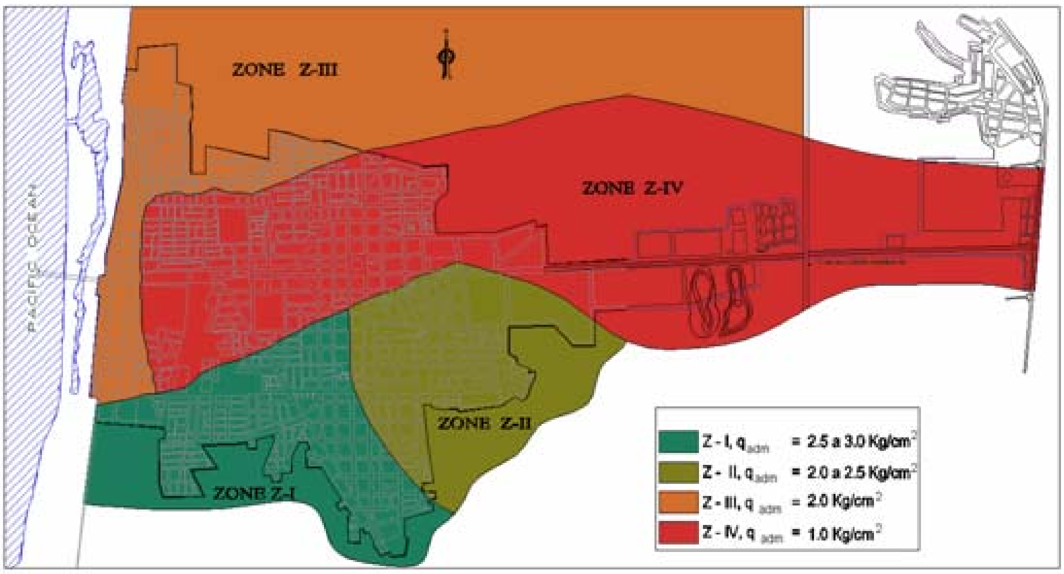

Fig. 3.35. Geotechnical zonation based on bearing capacity (Adapted from [13])

An updated version of the study mentioned before is presented by Aguilar et al, 2006 [7], whose work dealt with the estimation of the expected seismic amplifications. Fig. 3.36 shows three zones defined taking into consideration the geologic and geotechnical characteristics of soils. These three zones can be summarized as:

- Very high seismic amplification zone: Saturated lose sandy soils, with natural frequency periods greater than 1.4 sec that may amplify the bed-rock acceleration more than 3 times.
- High seismic amplification zone: Loose sandy and silty-sandy soils, slightly saturated with phreatic levels at 3.0 m depth. Natural periods between 1.2 and 1.4 sec that may amplify the bed-rock acceleration between 2.0 and 3.0 times.
- Intermediate seismic amplification zone: Sandy and gravely-sandy soils with medium levels of compaction, slightly saturated with phreatic levels at 3.0 m depth. Natural period around 1.2 sec and expected amplifications between 1.5 and 2.0.

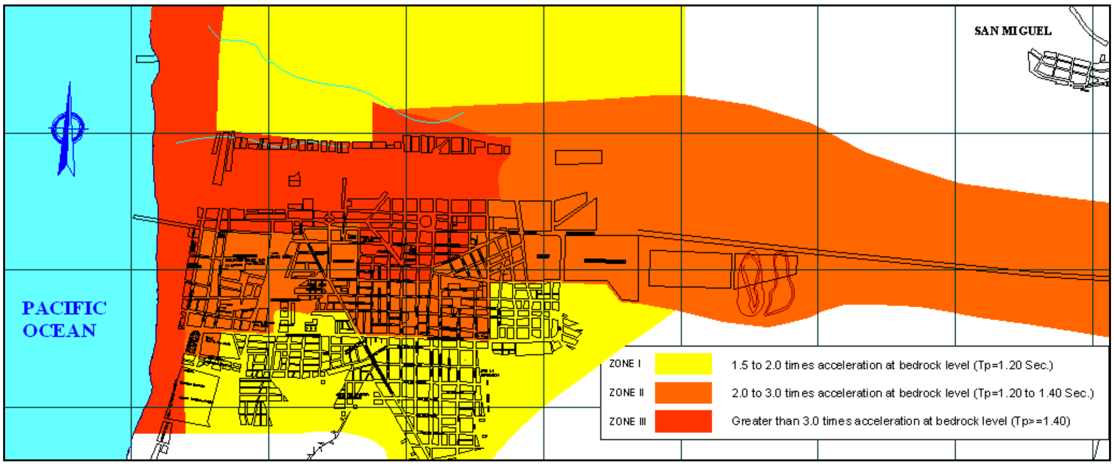

Fig. 3.36. Expected amplifications of seismic waves (Adapted from [7])

The distribution of amplifications across the city seems to follow the pattern of soil distribution, suggesting that the natural period and the expected amplifications might be based on the available information of soil characterization and phreatic level location.

Likewise, based on the information provided by the subsoil exploration, potentially liquefiable areas were identified using the method proposed by Seed et al, (1984).

Based on this, it was suggested that widespread liquefaction may take place along the coastline of Pisco. Partially liquefiable soils were identified in the northern part of the city, which corresponds to the oldest part of the city. (See Fig. 3.37)

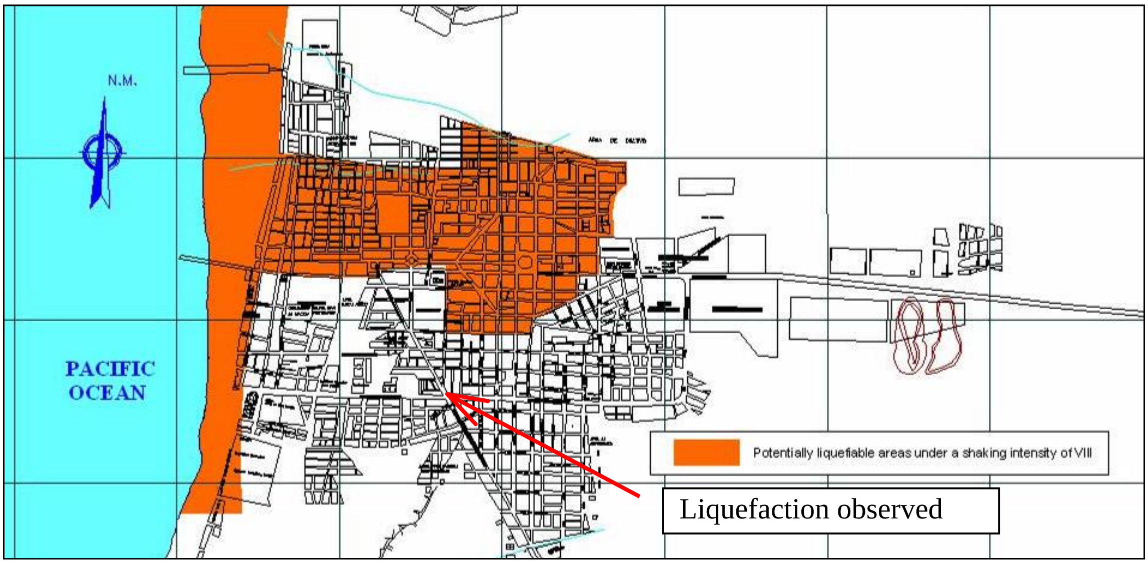

Fig. 3.37. Potentially liquefiable areas (Adapted from [7]). Liquefaction was observed outside this zone, one such location is indicated by the arrow and shown in Fig. 3.42.

Under the Sustainable City Program, which is managed by INDECI, a risk map, combining the potential effects of different hazards, such as floods, increments in phreatic level, earthquakes and tsunamis, was prepared. The Sustainable City Program aims at producing risk maps to guide the urban development of Peruvian cities. As of August 2007, maps for more than 120 cities have been produced. The risk map for Pisco City was prepared in association with the San Luis Gonzaga National University of Ica. In it, tsunami and flood hazards are considered more critical than liquefaction and ground motion amplification hazards.

Sanchez et al [17] also described the location of areas of waste disposal; some of them have been already urbanized while others might be used in future urban development. The characteristics of the deposits shown in Fig. 3.38 can be described as:

- Zone I: Located in the central and southern part of Pisco Playa. A lagoon left by the sea that later was leveled with debris aimed at future urbanization. Here soils are composed of crushed shells and construction wastes such as bricks, concrete, and sand
- Zone II: Southeast of Pisco. After being used for years as a sanitary filling, the current use of the area is the disposal of debris with similar characteristics to those of at Zone I.
- Zone III: East of Pisco. Leveled using the soil transported during the construction of the city's reservoir and the access road; nowadays it is a landfill occupied by factories and urban slums.
- Zone IV: Located in the Southern and Northern part of the coastline of Pisco, it has been filled with waste materials, but mostly, products of the fishing grounds and a variety of elements carried by sea currents.

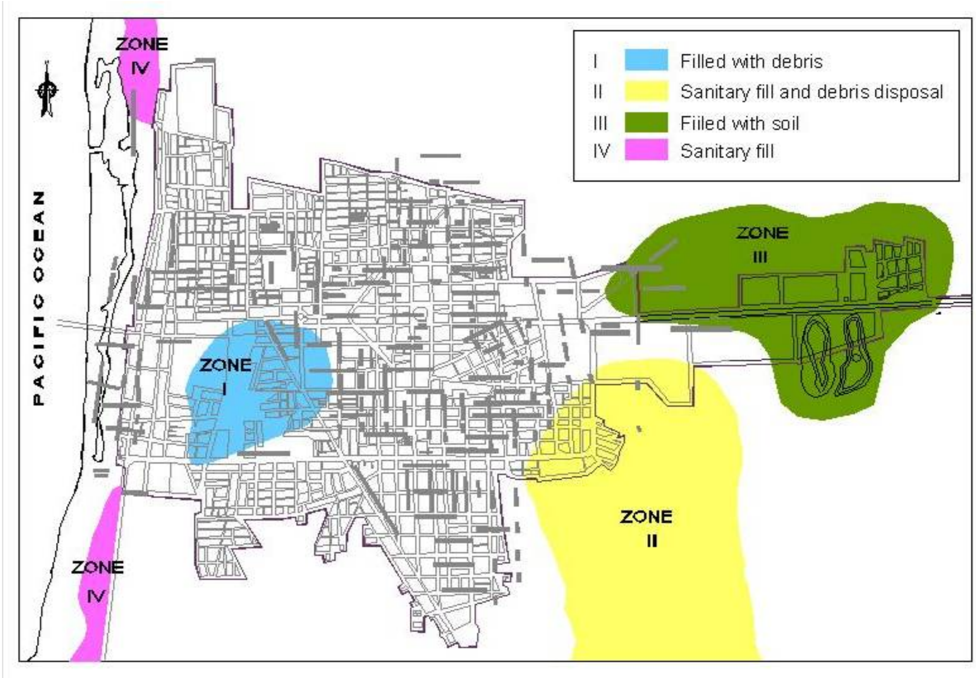

Fig. 3.38. Distribution of landfills in Pisco (Adapted from [13])

3.5.4. Overview of damage distribution

Evidences of soil deformation are clearly seen along the coast. However across the city it affected some buildings and other constructions. Areas close to the coastline particularly suffered extensive damage due to the shake but also, to the effects of the tsunami that hit the area minutes later. According to Barrientos [9], the run-up height of the wave estimated southwest of Pisco was 2.65 m.

The sewer system in Pisco, whose conditions were already poor before the earthquake, was drastically affected due to ground deformation and liquefaction. As shown in Fig. 3.39 and Fig. 3.40, central and southwest areas of Pisco had broken sewer pipes due to ground settlements and dislocated manholes were wide spread. Fig. 3.41 (Rodriguez et al [16]) also shows a lateral spreading movement along the coastline in the south of Pisco.

These points located along the coast and central part of Pisco, are within the area presented in Fig. 3.36 as prone to liquefaction. However, we observed liquefaction outside this “liquefiable zone” as indicated with an arrow in Fig. 3.36 and shown in Fig. 3.42. The extent of potentially liquefiable areas may deserve further review.

Fig. 3.39. Central Pisco (S13 42.542 W76 12.516). Settled ground as evidence of broken sewer pipes.

Fig. 3.40. Manhole pushed up and surrounded by ejected fine sand. Northwest of Pisco (S13 42.343 W76 13.029)

Fig. 3.41. Sub parallel cracks with lateral spread along the streets in the southwest of Pisco (Rodriguez et al [16])

Fig. 3.42. Liquefaction traces were observed north-west of the intersection between Valdelomar Street and Las Americas Avenue.

Agüero et al [6] has evaluated the macroseismic intensities based on the inspection of 30 buildings distributed throughout the city and using the MSK-64 scale adapted for Peru by Ocola (1979). Fig. 3.43 shows that high intensities are concentrated within the central part of the city, decreasing towards the south and southeast.

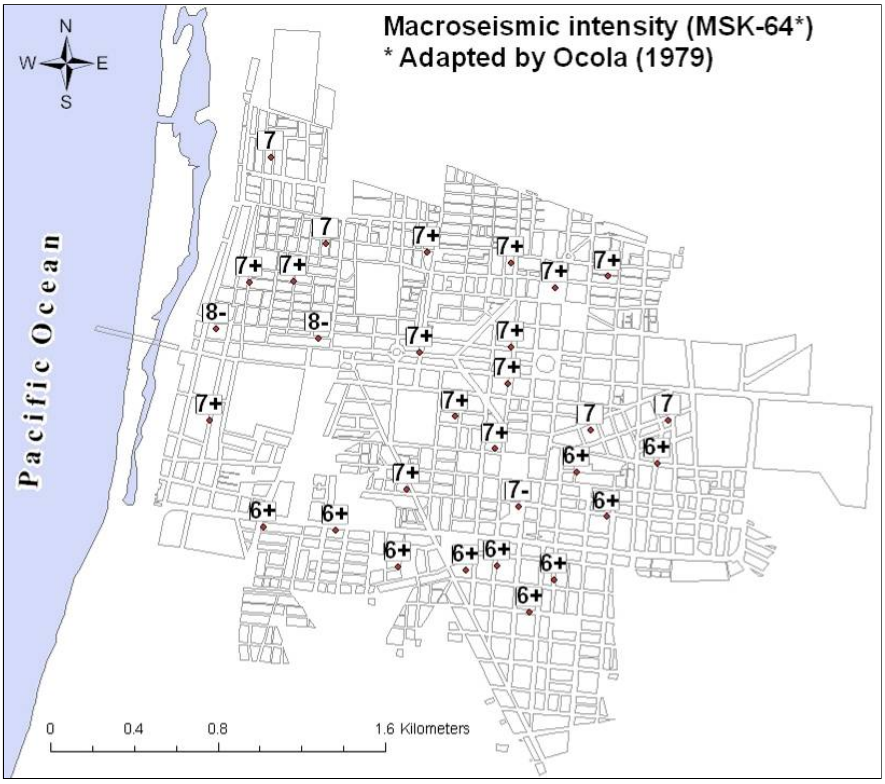

Fig. 3.43. Macroseismic intensity (MSK-64). (adapted from Agüero et al [6]

3.5.5. Microtremor measurements

We (hereafter UT) have collaborated with CISMID of the National University of Engineering (hereafter UNI) to perform a coarse microzonification of the city of Pisco (during September 15 and 16, 2007) with microtremor measurements at 34 different points in the city.

Both teams used a Geodas-10 recording equipment with CR-4.5-1 velocimeter (UNI) and CR-4.5-2S velocimeter (UT), The frequency range of 0.5-2.0 Hz for UT's velocimeters whereas 1.0-2.0 Hz for CISMID's It was defined that two sensors would be used at each point and all measurements should be 3 min long (100 Hz sampling frequency) and at least taken twice depending upon the surrounding conditions without initial filtering Before starting, sensors' response and recording parameters were a trial location.

We also performed microtremor array measurement at three locations (UNI one and UT two) across the city. We selected open areas free of topographic irregularities and evident sources of noise These data will be processed according the SPAC method [12]. Array layout and setup details are presented in Fig. 3.44 and Fig. 3.45.

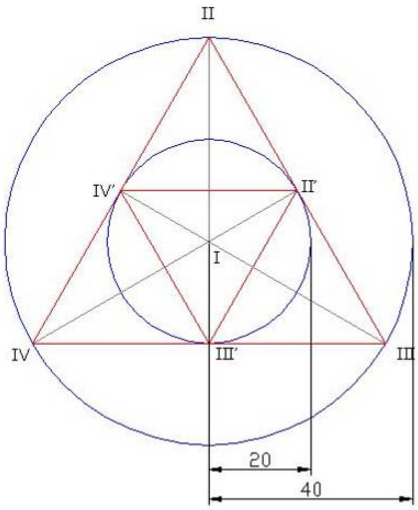

Fig. 3.44. Array for SPAC measurements. (Radii in meters)

Fig. 3.45. Open areas chosen for SPAC measurement. Below the tripod is the central sensor. (Labeled as I in Fig. 3.44)

Fig. 3.46shows the test's location, measurements taken by CISMID and UT teams are represented as red a blue dots, respectively. Also, triangles were used to identify the SPACs taken by the UT.

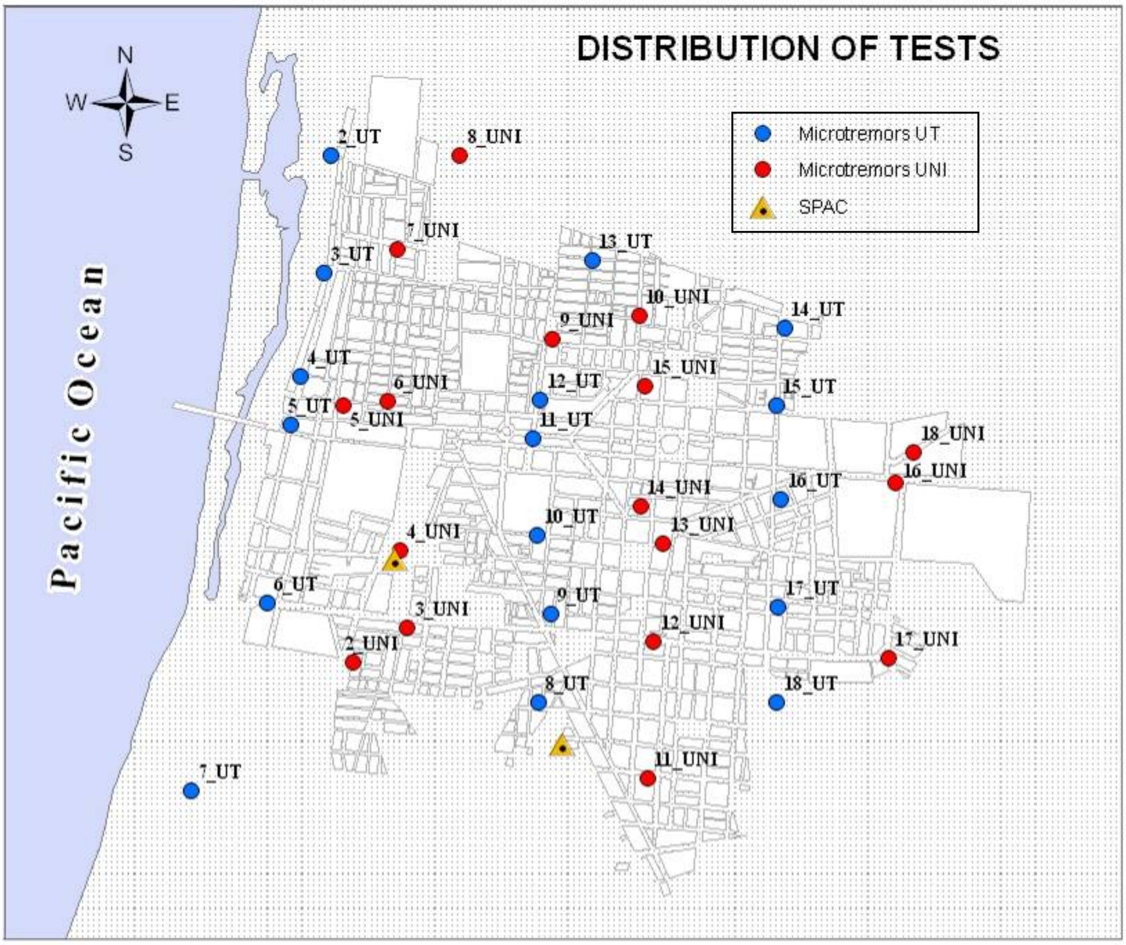

Fig. 3.46. Location of test conducted by CISMID and the University of Tokyo

Fig. 3.47 to Fig. 3.54 summarize additional comments on the surrounding conditions where microtremors were conducted. Highly contrasting characteristics between almost flat areas due to severe damage in the west side whereas scattered collapsed and less affected houses towards the east.

Fig. 3.47. (Point 2_UT) The number of standing buildings is small, high level of damage.

Fig. 3.48. (Point 5_UT) At San Martin Av. where many nearby adobe houses were about to collapse

Fig. 3.49. (Point 7_UT) In front of the beach "Camino San Andres". Non-inhabited area.

Fig. 3.50. (Point 13_UT) Less affected area with one and two story houses almost undamaged

Fig. 3.51. (Point 11_UT) At the intersection with San Martin Av, close to

Fig. 3.52. (Point 8_UT) In front of Communal gathering place. Few damages

Alexander Humbolt School. Few collapsed houses, debris deposited on the left side of the road.

in surrounding structures.

Fig. 3.53. (Point 15_UT) Two blocks from the main square. Contrasting large amounts of debris from nearby collapsed buildings on the right side while almost undamaged houses on the left.

Fig. 3.54. (Point 17_UT). Less evident damage. However, one block northwards there was a totally collapsed adobe house, and a masonry house less severely damaged but it underwent large settlements due to soil deformation.

3.5.5.1. Results

In order to be consistent all the data was processed with same criteria using the software Geopsy [2] and Fig. 3.55 shows the H/V ratio determined frequencies for all points. 11 out 34 points did not show any clear peak, e.g. the zone of amplification was too broad to distinguish a peak, or the peak was split into two or three parts, or the amplification was less then 2. Examples of these three categories can be found in Fig. 3.56. Out of the remaining 23 points, 6 points had frequency peak beyond the sensor range, however may be accepted to a certain level since we are using the ratio of the horizontal and vertical fourier spectra. Furthermore, for neighbouring locations with such high frequencies, we obtained similar results to the UNI team.

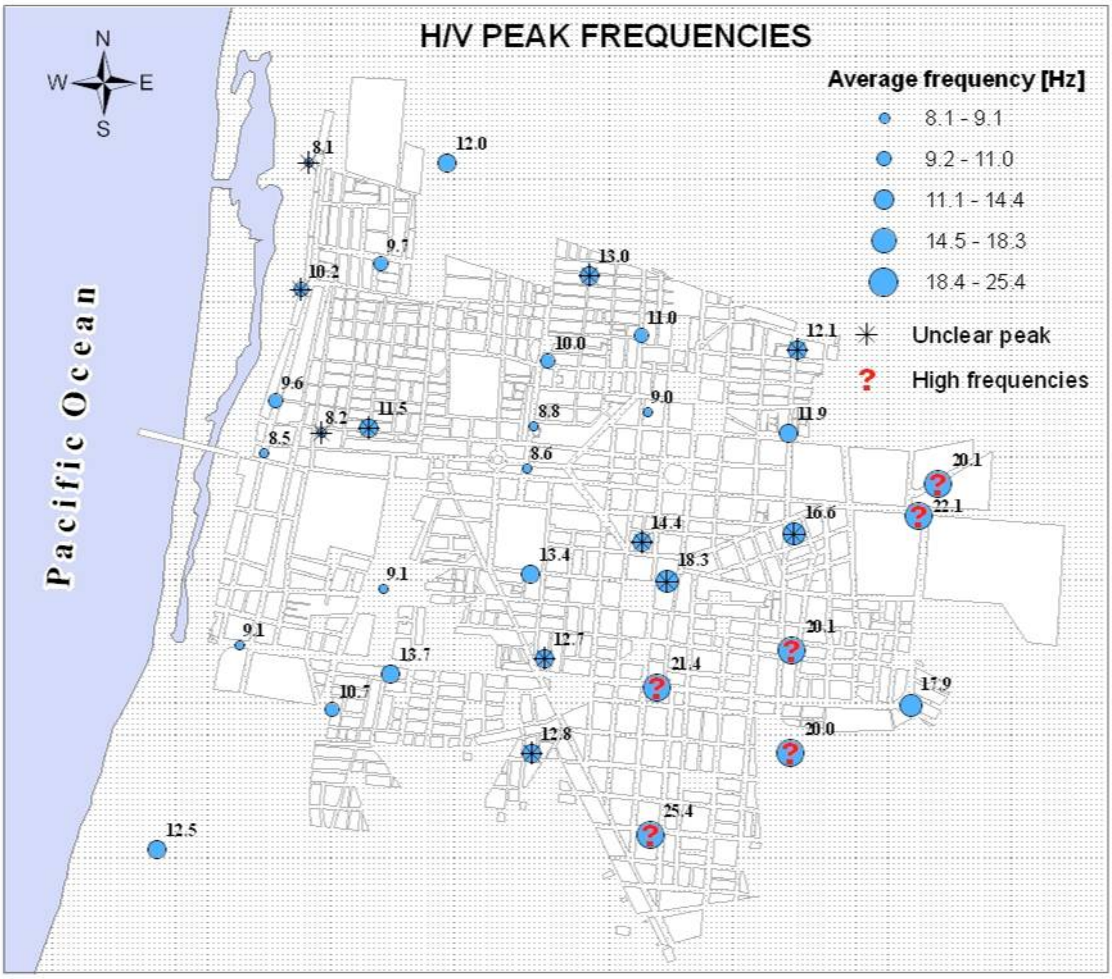

Fig. 3.55. H/V peak frequencies

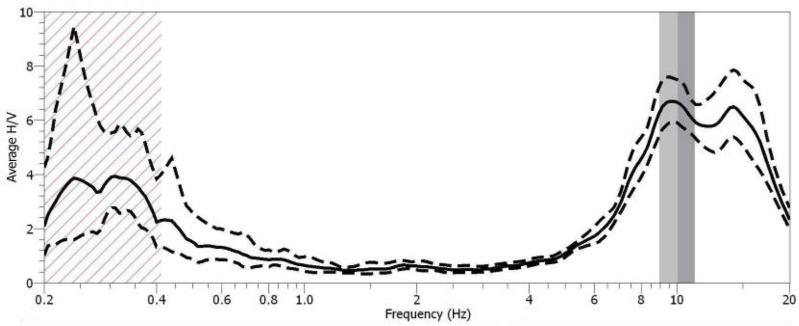

(a)

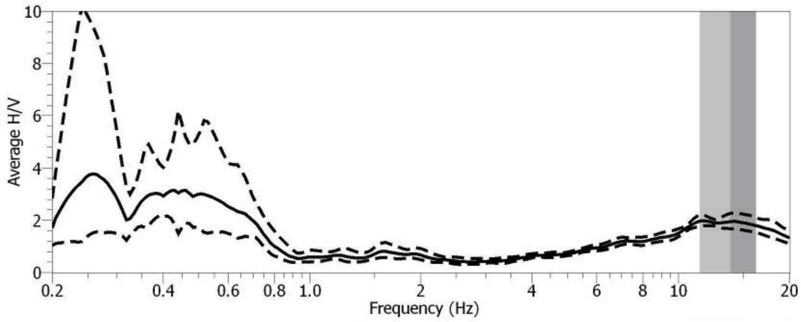

(b)

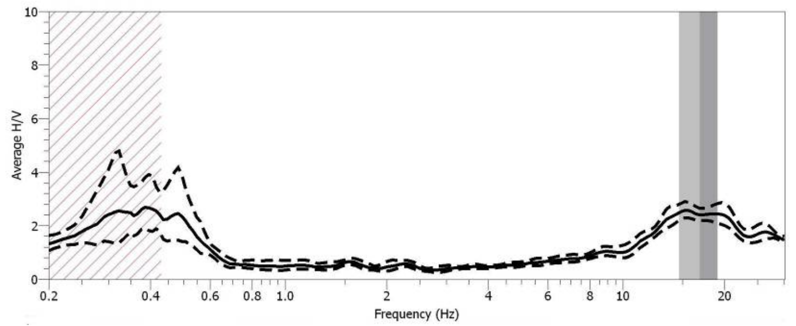

(c)

Fig. 3.56. Examples of H/V spectral ratios regarded as non reliable

a. *Pont ID: 6_UNI. Clear amplification but the peak is split into two parts having similar amplitudes.*
b. *Point ID: 8_UT. Low amplification*
c. *Point ID: 13_UNI. Amplification exists but the possible range is too broad to pick up one single frequency*

Keeping that in mind, Fig. 3.57 presents the data using blue circles for easily identified peaks while the red one represents those difficult to identify. Based on the reliable points, a straightforward spline-type interpolation was made aimed at depicting the general trend of the peak frequencies. These results suggest that there is a North-West to South-East trend of increasing frequencies .

However, this interpolation should be further studied in combination with available soil classification, SPT data, and an updated lithological map (INGEMMET, work in progress).

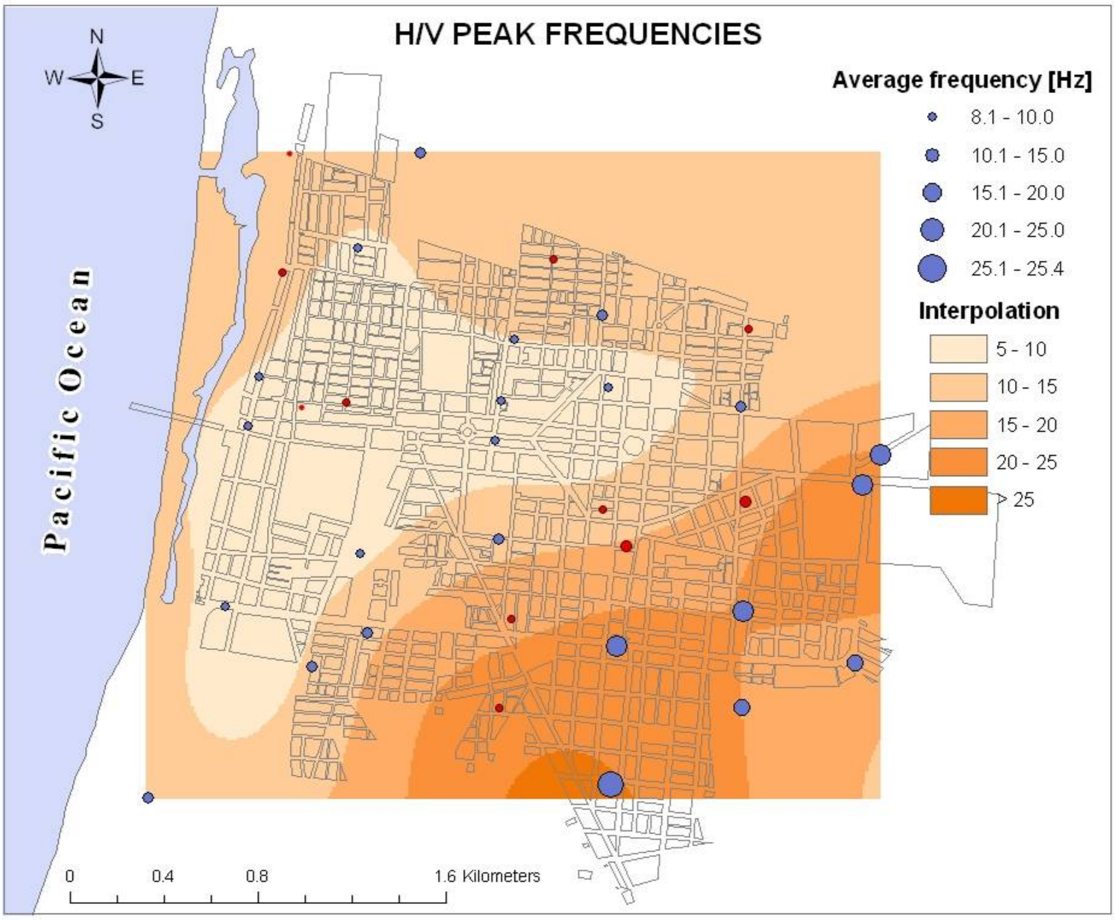

Fig. 3.57. H/V peak frequencies. Local values and contours.

Fig. 3.58 shows the local values of peak amplitudes, using asterisks (with amplification values) to mark the location of points for which it was difficult to identify the peak, while a question mark for those points where the peak frequency is out of the sensor range.

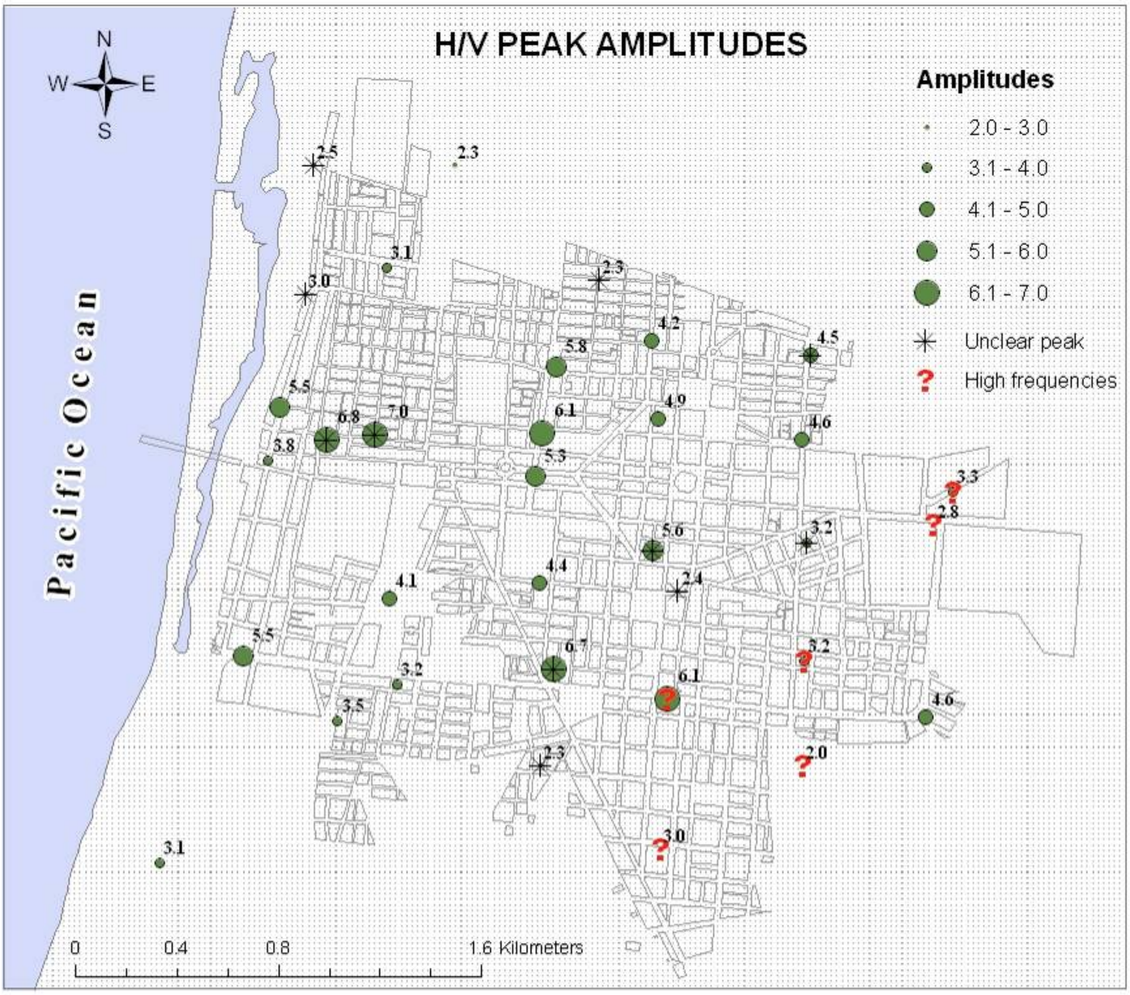

Fig. 3.58. H/V peak amplitudes

Fig. 3.59 shows the interpolated contours. It is difficult to identify a general pattern and the influence of the non-reliable points may change the geometry of these contours, thus stressing on the necessity of a denser mesh of measurements.

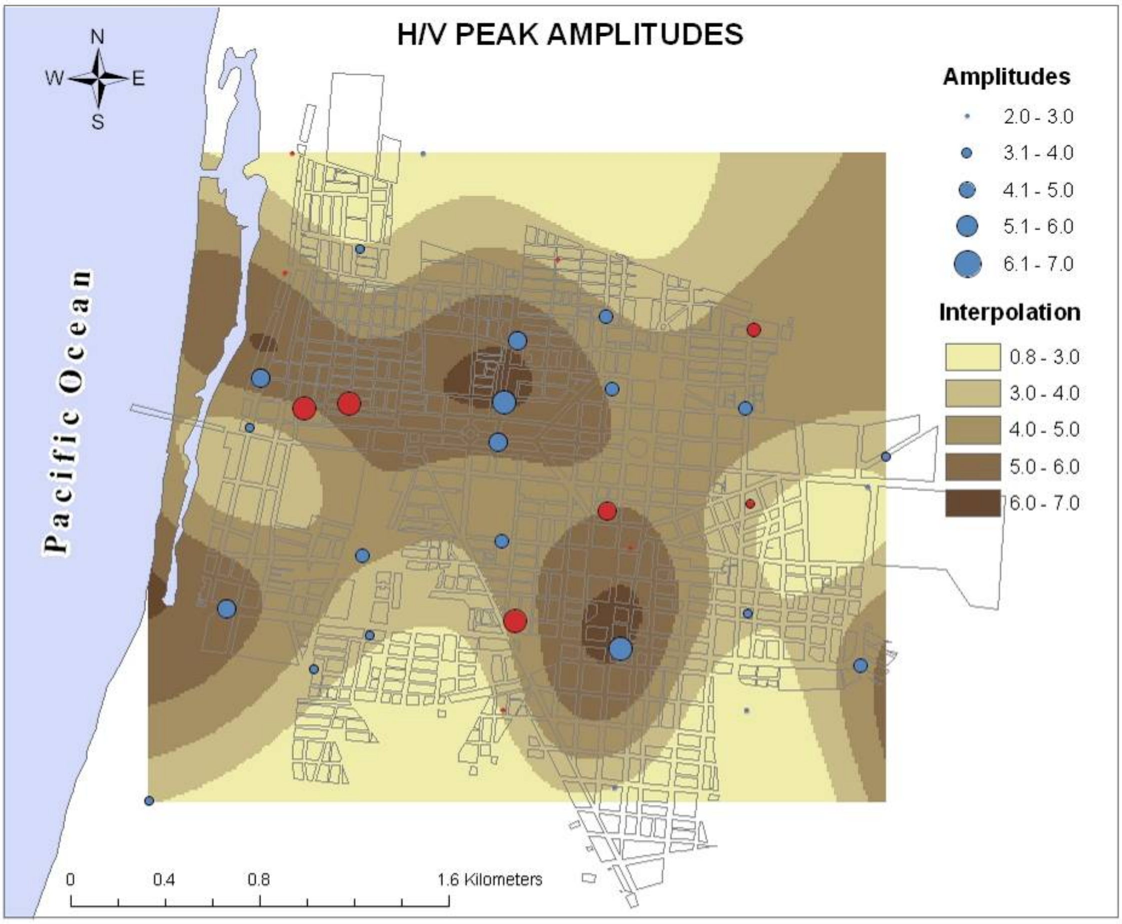

Fig. 3.59. H/V peak amplitudes. Local values and contours.

3.5.6. Discussion

By comparing the results presented in 3.5.3 with those described in 3.5.3, the following comments can be made:

- Stiffer soil and/or zones with thinner soft soil cover seem to be located in the southeast of Pisco, and it agrees to some extent with the geotechnical zonation in Fig. 3.35.
- The northern 1.2 m deep deposit of sandy clay overlying the averaged 3 m deep deposit of silty sand (identified as Zone III in Fig. 3.35) shows low frequency values whereas the south eastern deposit (identified as Zone II) having the same soil classification and depths of 0.5 and 1.1 respectively, exhibit higher frequencies; showing the effects of thickness in the H/V peak frequency.
- In the west side, the combined effect of deposit stiffness and thickness hinders the interpretation of frequencies, showing similar frequencies in the averaged 1.2 m deep deposit of clay and rounded gravel (identified as Zone IV in Fig. 3.35) and the deep deposit of gravel located in the south (referred as Zone I).

Regarding H/V maximum amplitudes, there is a sort of good agreement between the areas of maximum expected amplification in Fig. 3.36 and the H/V peak amplitudes of microtremor measurements (Fig. 3.59). Maximum values are close to the coastline and extend toward the east along the centre of Pisco, though there some areas of concentration of higher values in the southeast.

The local high value obtained at the old sanitary fill in the southeast side deserves further analysis (classified as Zone II Fig. 3.38 in), especially if this area is located in an area towards which the city is growing.

Finally, the data provided by Agüero et al [6] were plotted overlapping the peak amplitudes in Fig. 3.60. Despite of the fact that the microtermor data describe partially characteristics of the ground, while the macroseismic intensity encompasses the combined effect of building damage, ground deformations and people's perception; there is some consistency in terms of the high values observed in central and southeast Pisco in both studies. Nevertheless, it ought to be emphasised that additional site response estimations are required.

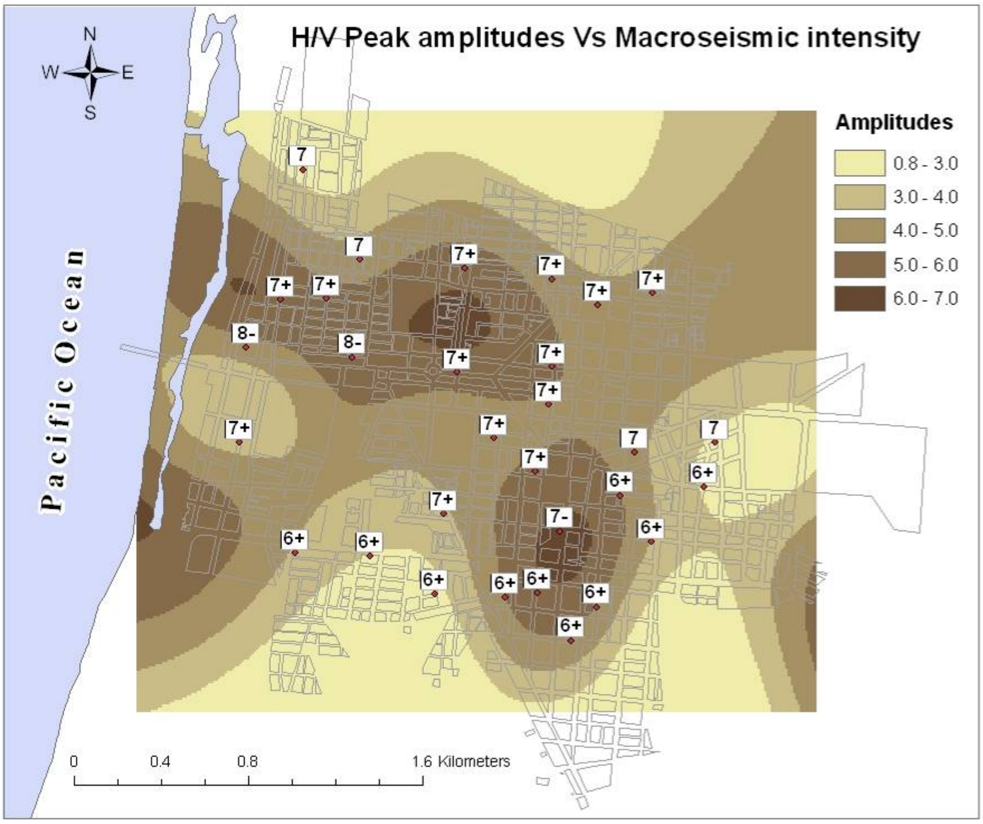

Fig. 3.60. Contours of H/V peak amplitudes and Macroseismic intensity (MSK-64, Adapted from[6].)

3.6. Conclusions and recommendations

Below follows some conclusions and recommendations based on the several examples of observed geotechnical and foundation related damages give above.

Liquefaction induced large soil cracks and displacements were observed in Tambo de Mora and Pisco. The only way to reduce the damages induced by such soil deformations is with reinforced strong, and expensive, foundations. The good performance of such foundations were clearly shown by a newer school house in Tambo de Mora and a Hotel in Pisco. The strong foundations are especially important for public buildings like schools and hospitals. Weak foundations, similar to the one of the health center in Huaytara, needs to be retrofitted or reconstructed.

In many locations we observed moist adobe walls due to the lack of foundation preventing moisture from entering the walls from the surrounding ground. In addition to reducing the earthquake resistance of an already earthquake vulnerable building type, the moisture also constitute a general health problem.

It is not easy to reduce the effects of large soil cracks, such as the ones observed in Nuevo Monte Rico. With strong reinforced foundation slab houses may have withstood some of the deformations, however rotation and or rocking of the foundation is still very likely, but people would be able to escape.

The cracks in the field are impossible to prevent. However, they can be filled up with coarser material (boulders, pebbles, gravel) and then covered with finer material (sand, clay, agriculture soil) as to allow for irrigation without “leakage” of to much water into the cracks. The wells that went dry, may become filled up again, however it the water level change is permanent then it is likely that the acquifer conditons changed and new well have to be dug/drilled. Emergency tanks could be one way provide water in case of a disaster.

While it may take time, it is very important to base the land use plans on existing hazard maps. The damages in Tambo de Mora and Pisco coincide very well with these maps, showing their importance. (Once such maps are updated, land use laws can also be updated.)

REFERENCES

[1] INGEMMET: Geological map, quadrangle 27k, 1999
[2] http://www.geopsy.org/
[3] INEI (National institute of statistics and information): www.inei.gob.pe, Census 2005.
[4] INDECI (National Institute of Civil Defense): http://www.indeci.gob.pe/
[5] Seismic Hazards map of Chincha. Program of Sustainable Cities. Institute of National Defence (INDECI) – National University of ICA (UNICA). 2001 Available on www.sinadeci.indeci.gob.pe/PortalSINPAD/Mapas_Catastral/Mapa_Peligro_Chincha.pdf
[6] Agüero C, Tavera H, Fernandez E, Huaco P, Talavera C and Arredondo L. Macrosesismic intensities in the urban area of Pisco regarding the earthquake of August 15, 2007. Preliminary version. Geophysical Institute of Peru. Available on http://khatati.igp.gob.pe/Webs/cns06/pisco2007/terremoto_pisco_2007.htm (in spanish)
[7] Aguilar Z. Geotechnical microzonation of Pisco. National University of Engineering. Lecture on Disaster management for sustainable development. Territorial Studies. 2006. Lima, Peru.
[8] Astroza M. Intensities and earthquake induced damages. Report on affected areas by the earthquake of August 15th, 2007. Available on http://www.ceresis.org/informacion/ (In Spanish)
[9] Barrientos S. Report of the August 15th, Tsunami run-up heights induced by the Mw=8.0 earthquake of august 17, 2007, Pisco, Peru. Available on http://www.ceresis.org/informacion/ (In Spanish)
[10] Marc Wathelet. Geopsy software. Version 2.0.0-Beta. Available on www.geopsy.org

[11] National Institute of Civil Defense. Annex of emergency report No 336 "Ica and South of Lima departments severely affected by seismic movement".. Available on www.indeci.gob.pe. (In Spanish).
[12] Okada H. The microtremor survey method. Geophysical monograph series. Society of exploration geophysicists. Number 12. 2003
[13] Parra D, Vasquez D, Alva J. Geotechnical microzonation of Pisco. Proceedings of the 12th National Symposium on Civil Engineering. November, 1999. Lima, Peru. (In Spanish).
[14] Pierre-Yves Bard (Project Coordinator). Guidelines for the implementation of the H/V spectral ratio technique on ambient vibrations. Measurements, processing, and interpretation. December 2004. Available on http://sesame-fp5.obs.ujf-grenoble.fr/Papers/HV_User_Guidelines.pdf
[15] Program of Sustainable Cities. Institute of National Defence (INDECI) – National University of ICA (UNICA). 2001. Hazards map of Pisco. Available on http://sinadeci.indeci.gob.pe/PortalSINPAD/Mapas_Catastral/Mapa_Peligro_Pisco.pdf
[16] Rodriguez L, Dominguez J, Lopez R., Rendon H. Post-seismic evidences of geologic instability.. Venezuelan Institute of Seismological Investigations (FUNVISIS) Available on http://www.ceresis.org/informacion/ (In Spanish)
[17] Sanchez M, Parra D, De la cruz K.Seismic microzonation of Pisco city. CISMID-UNI Geotechnical laboratory. 1999 (In Spanish).